Letters in Applied NanoBioScience
Open-Access Journal (ISSN: 2284-6808)

Article
Volume 13, Issue 1, 2024, 31
https://doi.org/10.33263/LIANBS131.031

Green Synthesis of Silver and Copper Nanoparticles for Potential Biopesticide Application Against Oriental Fruit Fly (*Bactrocera dorsalis* Hendel)

Danila S. Paragas [1,*], Jay-Lord P. Viloria[1,2]

[1] Department of Chemistry, College of Science, Central Luzon State University, Science City of Muñoz, Nueva Ecija, Philippines
[2] Pangasinan Safe Water Laboratory, Inc.; #375 Tobor, Malasiqui, Pangasinan, Philippines, jpviloria.chem@gmail.com (J.P.V.)
* Correspondence: danilaparagas1010@clsu.edu.ph (D.S.P.);

Scopus Author ID 57217117318
Received: 6.01.2023; Accepted: 22.02.2023; Published: 13.08.2023

Abstract: Background: The fruit fly species *Bactrocera dorsalis* (Hendel) is one of the most severe pests affecting most tropical countries' agricultural fruits.The green synthesis of silver and copper nanoparticles from plant extracts is aimed at determining the potential application of nanoparticles against *B. dorsalis*. Methods: Silver (AgNPs) and copper nanoparticles (CuNPs) were synthesized from reacting $AgNO_3$ and $CuSO_4.5H_2O$, respectively, with *Cymbopogon citratus* and *Tridax procumbens* extract.Optimization was done by varying the reaction mixture's volume ratio, pH, and temperature. The percent mortality of fruit flies was evaluated after progressive exposure to AgNPs and CuNPs. Results: The formation of AgNPs and CuNPs using plant extracts is favorable in alkaline conditions - pH 11 (*C. citratus*) and pH 9 (*T. procumbens*) extract, requiring 50ºC for AgNPs, and <70ºC for CuNPs. AgNPs and CuNPs in agglomerates have approximate sizes of 70 nm and 57 nm, respectively. *T. procumbens*-AgNP exhibited the highest anti-fruit fly activity, causing 66.7 ± 23.1% mortality. AgNPs have significantly improved the two plant extracts' insecticidal activity, while CuNPs have caused no mortality. Conclusion: This study further proves the effectiveness of AgNPs in pest control.AgNPs can be incorporated into bait stations using natural attractants to prevent environmental concerns.

Keywords: biopesticide; environment-friendly; fruit fly; nanoparticles; pest.

© 2023 by the authors. This article is an open-access article distributed under the terms and conditions of the Creative Commons Attribution (CC BY) license (https://creativecommons.org/licenses/by/4.0/).

1. Introduction

The fruit fly species *Bactrocera dorsalis* (Hendel) has been identified as the primary pest of mangoes other than *Bactrocera carambolae* [1]. *B. dorsalis* is widely distributed in the Asia Pacific and Africa [2]. *B. carambolae* has narrower distribution in Southeast Asia and has recently been introduced to South America [3]. Populations of these fruit fly species increase from October to December, which decreases from February to June [1].

Chemical pesticides, a traditional control measure, impose hazards by exposure to various sources in which pesticide residues are found, such as food and water; garden and lawn use; farm use; and occupational exposures [4]. Contact with the active chemical components of pesticides, such as organophosphates and carbamates, can cause cardiovascular and respiratory diseases, skin cancer, hearing loss, and amputations [5]. Thus, developing other methods concerning environmental and public health risks is necessary.

Physical control methods such as Eco-Trap mass control [6], hybrid biological and chemical control techniques [7], and augmentoria [8] were used. Augmentoria is a technique defined as a tent-like structure designed to sequester tephritid flies emerging from infested fruits. *Bacillus thuringiensis* biopesticide [9] and fungal-based biopesticide *Beauveria bassiana* [10] were also applied in sustainable agriculture. The use of spray baits containing protein hydrolysates [11], ammonia salts, and Torula yeast [12] have also been considered as alternatives.

Moreover, the use of nanopesticides for pest management has emerged due to the increasing popularity of research in nanotechnology for agricultural applications [13-16]. Nanopesticides contain either tiny particles of pesticidal active ingredients or nanoscale materials with beneficial pesticidal properties [17,18]. Nanomaterials show valuable properties such as permeability, thermal stability, solubility, and biodegradability, which are required in formulating nanopesticides [19]. Also, due to the large surface area of nanomaterials, the affinity to the target pest is more significant than most common pesticide active ingredients [20].

Nanoparticles were commonly produced by physical and chemical methods such as ion sputtering, solvothermal synthesis, reduction, and sol-gel technique [21,22]. A green process, which involves plant extracts from lemongrass and tridax daisy as reducing agents, is applied in synthesizing silver and copper nanoparticles. Plant extracts from lemongrass and tridax daisy are viable options since they are freely available and widespread plants in the country. Therefore, using these plants for synthesizing nanoparticles is an innovative application. This synthesis method is chosen to complement the formulation of nanopesticide for oriental fruit fly suppression with little to no undesirable environmental effects.

2. Materials and Methods

2.1. Chemicals and reagents.

The following analytical grade chemicals were used: $AgNO_3$, $CuSO_4 \cdot 5H_2O$, and NaOH. All glassware was cleaned and acid-washed, followed by rinsing with distilled water.

2.2. Plant materials preparation.

The leaves of *Tridax procumbens* (tridax daisy) and *Cymbopogon citratus* (lemongrass) were collected at Central Luzon State University, Science City of Muñoz, Nueva Ecija, Philippines. The leaves were detached from the stems and washed with distilled water. The fresh leaves were stored in a clean, covered container.

Coconut water was used as the solvent for plant extraction. The coconut water collected was filtered using ordinary filter paper to remove the solid particles. It was then placed in bottles and stored in the refrigerator until use.

2.3. Plant extraction.

Extraction of the leaves from the plants was done by boiling the coconut water and then adding the fresh-cut plant leaves with a ratio of 400:100 milliliter of solvent to gram of lemongrass and tridax daisy. The extraction ratio of lemongrass and tridax daisy was based on the study of Masurkar *et al*. [23] and Bhati-Kushwaha and Malik [24], respectively. Boiling the leaves was done for five minutes. After cooling to room temperature, the extract was filtered

using Whatman No. 1 filter paper to remove the solids.The extract was then placed in an amber bottle and stored in the refrigerator until use.

2.4. Synthesis of metal nanoparticles and optimization of parameters.

One millimolar of $AgNO_3$ and $CuSO_4.5H_2O$ were used to synthesize AgNPs and CuNPs by reduction reaction using the two plant extracts. A change in color from yellow to reddish-brown indicated the reduction of Ag^+ to Ag^0 and Cu^{2+} to Cu^0.

The synthesis of metal nanoparticles was optimized by varying the volume ratio, pH, and temperature of the plant extract mixture and working solutions ($AgNO_3$ and $CuSO_4.5H_2O$). Volume ratios of 10:90, 20:80, and 30:70 (V1, V2, V3) of the lemongrass extract and tridax daisy extract to $AgNO_3$ and 50:50, 60:40, and 70:30 (V1, V2, V3) of the lemongrass extract and tridax daisy extract to $CuSO_4.5H_2O$ were used. In each ratio, optimization of pH and temperature was done. In four 100-mL beakers containing a constant specific volume of the extract (based on each volume ratio), the pH of the three extracts was adjusted to 7, 9, and 11 (P1, P2, P3), respectively, using 0.01M NaOH.In contrast, the initial pH of one extract was kept unchanged. After changing the pH, a corresponding $AgNO_3$/$CuSO_4$•$5H_2O$ (based on each volume ratio) was added to the extract, and the mixture was shaken. Each mixture's initial wavelength scan (300-800 nm) was done using a UV-Visible Spectrophotometer (Hitachi U-2900 model). In three 10-mL test tubes, each mixture with different pH was transferred into the tubes (filled up to approximately three-fourths of the test tube). The three test tubes were subjected to 50ºC and 60ºC water baths (T1, T2) for the silver nanoparticle synthesis, while 70ºC and 80ºC water baths (T1, T2) for the copper nanoparticle synthesis. A wavelength scan of all the mixtures with different parameters was made after one hour of reaction.

The optimum treatment for synthesizing AgNPs and CuNPs in each plant extract was determined by wavelength scan. The absorbances of parameters showing a peak within the 400-440 nm range (for AgNP) and 560-600 nm (for CuNP) were compared and subjected to one-way Analysis of Variance (ANOVA). Generally, the parameter with the spectrum showing the highest absorbance was considered the optimum parameter.

2.5. Characterization of synthesized nanoparticles.

Surface plasmon resonance (SPR) spectra of the synthesized nanoparticles were obtained from a UV-Vis spectrophotometer at 400-440 nm for AgNPs, and 560-600 nm for CuNPs. The nanoparticles were further characterized using scanning electron microscopy (SEM) for surface morphology. In drying nanoparticles for the SEM analysis, the stored supernatant solutions were oven-dried at 50ºC for 12 hours. The collected dried nanoparticle scrapes were kept in small, capped polyethylene tubes.

2.6. Insecticidal treatments.

Male oriental fruit flies were collected in mango plantations at the Central Luzon State University by trapping them using methyl eugenol as an attractant. Assessment of the mortality rate of fruit flies using the insecticidal treatments was done by isolating the flies in a transparent plastic container. A circle, three inches in diameter, was cut from the plastic container's cover and replaced by silk for the flies to maintain a suitable atmosphere. In the laboratory, the temperature condition was at room temperature (30ºC).

The insecticidal treatments used are the plant extracts and plant extracts-metal nanoparticles suspension. Triplicate set-ups were done for the anti-fruit fly application. Ten drops of the extracts and nanoparticle suspension were used. The treatments were dropped onto a small piece of cotton placed at the center of the container's cover. The mortality of the fruit flies was assessed after the first contact with the treatment and was updated after 0.5, 1, 2, 4, 6, 8, and 12 hours. The percent mortality recorded for each treatment was analyzed using a one-way Analysis of Variance (ANOVA).

3. Results and Discussion

3.1. Preliminary synthesis of metal nanoparticles.

3.1.1. Silver nanoparticles.

Silver nanoparticles (AgNPs) were successfully synthesized by the reaction of $AgNO_3$ and reducing constituents from lemongrass and tridax daisy extracts. The resulting red-brownish color of the suspension indicates the formation of silver nanoparticles by reducing Ag^+ to Ag^0 [24]. The color change observed in the suspension (Figures 1C and 1D) is due to the surface plasmon resonance (SPR) of metal nanoparticles which is brought by the interaction of light incident on the nanoparticle surface with the conduction electrons of the metal [25].

UV-Visible spectroscopy was used to attest to the formation of AgNPs. The distinctive peak observed in the UV-Visible spectra of the silver salt-lemongrass nanoparticles suspension (LG-AgNP) at 400 nm with an absorbance of 1.226 (Figure 1A) is a characteristic peak of AgNP spectra [26]. A broad peak detected in the UV-Visible spectra of silver salt-tridax daisy (TD-AgNP) suspension at 413 nm with an absorbance of 0.506 also indicates the formation of AgNPs but of more dispersed size due to the band broadening.

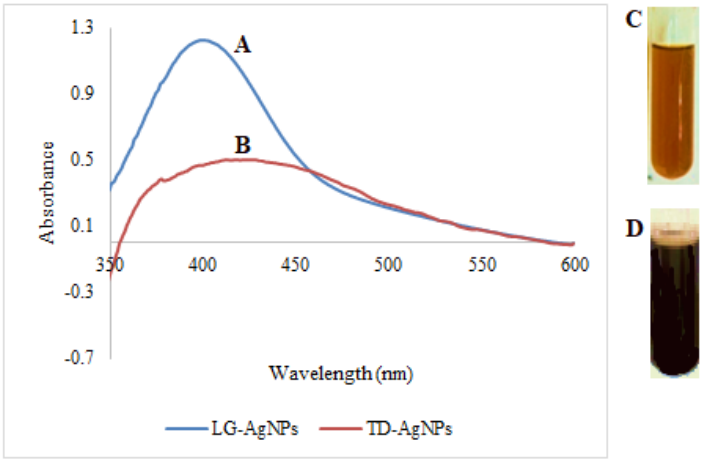

Figure 1. UV-Visible absorption spectra of (A) lemongrass-synthesized AgNPs (LG-AgNPs) and (B) tridax daisy-synthesized AgNPs (TD-AgNPs) and color observed after the formation of AgNPs using (C) lemongrass extract and (D) tridax daisy extract.

3.1.2. Copper nanoparticles.

The appearance of the brownish color of the reaction mixtures using the lemongrass and tridax daisy extracts due to the excitation of surface plasmon is characteristic of the formation of copper nanoparticles (CuNPs) [27]. The UV-Visible spectrum shows an absorbance maximum at 580 nm for the tridax daisy-synthesized CuNPs (Figure 2A-1) and a

weak absorbance peak at 585 nm for the lemongrass-synthesized CuNPs (Figure 2B-1) in which the formation of CuNPs can be further confirmed [28].

An absorbance peak at 428 nm (Figure 2B-2) in the spectra of lemongrass-synthesized CuNPs, and 452 nm (Figure 2A-2) in the spectra of tridax-daisy-synthesized CuNPs indicates the formation of Cu_2O, which implies that the reduction is incomplete [29], or the stabilizing and capping ability of the extract is low. Furthermore, Chen *et al*. [30] reported that these absorbance peaks within 400-450 nm indicate the formation of Cu_2O nanocubes, as seen in the Transmission Electron Microscope (TEM).

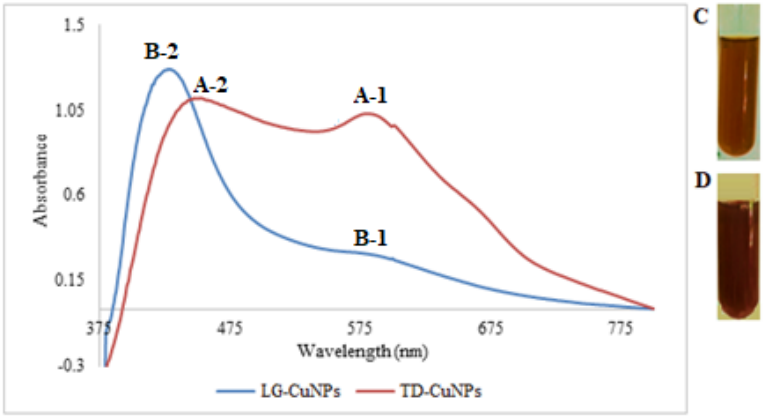

Figure 2. UV-Visible absorption spectra of (A) lemongrass-synthesized CuNPs, and (B) tridax daisy-synthesized CuNPs, and color observed after the formation of CuNPs using (C) lemongrass extract, and (D) tridax daisy extract.

3.2. Optimization of parameters.

3.2.1. Silver nanoparticles.

The effect of the volume ratio of plant extract to a salt solution, pH, and temperature in the synthesis of AgNPs was evaluated based on SPR spectral changes. The optical properties of metal nanoparticles strongly depend on the nanoparticles' size, shape, composition, structure, and adsorption layers [31]. Therefore, absorption spectra can be used to evaluate the effects of different optimization parameters.

Table 1. Absorbances of AgNP from lemon grass and tridax daisy extracts.

Parameters		LG-AgNP*	TD-AgNP^{ns}
Volume Ratio	V1 (10:90)	0.578^{b}	0.563
	V2 (20:80)	41.331^{ab}	0.506
	V3 (30:70)	1.647^{a}	0.552
pH	P1 (7)	0.447^{b}	0.499
	P2 (9)	0.578^{b}	0.543
	P3 (11)	1.127^{a}	0.506
Temperature	T1 (50°C)	1.644^{a}	0.485
	T2 (60°C)	1.528^{a}	0.394

* - absorbances in a column per parameter followed by the same letter superscript are not significantly different at 5% level.

The absorbances of silver nanoparticles synthesized from the lemongrass and tridax daisy extracts as affected by the different parameters are presented in Table 1. Three volume ratios of plant leaf extracts to $AgNO_3$ solution were used. The SPR spectra of AgNPs change with the various volume ratios and are shown in Figure 3.

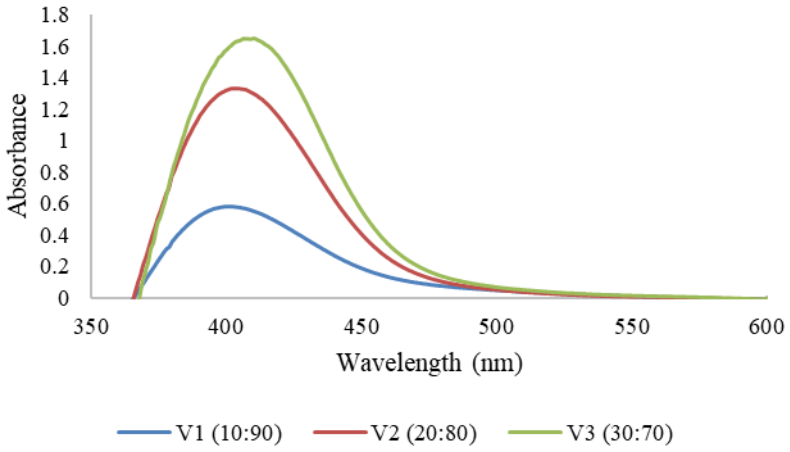

Figure 3. Effect of volume ratio of lemongrass extract to 1mM $AgNO_3$ solution on AgNPs formation.

In the lowest ratio (V1, 10:90) using lemongrass extract (Figure 3), a relatively broad SPR peak at 401 nm was observed after an hour of reaction of the mixture. Increasing the ratio to 20:80 (LG: $AgNO_3$) resulted in a more intense color change from yellow to yellowish-brown and exhibited a more prominent absorption peak at 403 nm. Furthermore, the optimum ratio (30:70) was the highest, which produced the most intense brownish solution, and exhibited the highest absorbance (1.647) among the three ratios. However, the absorbance maximum shifted to 410 nm. Generally, shifting the peak to a higher wavelength, or redshift, indicates a larger metal nanoparticle produced than a shorter wavelength [26]. Statistically, V3 was more effective than V1 in generating the SPR spectra with the highest absorbance. However, the absorbance shown by V3 is significantly the same as of V2, but still, V3 is the optimum ratio since it has generated the highest absorbance peak at 400-440 nm (Table 1).

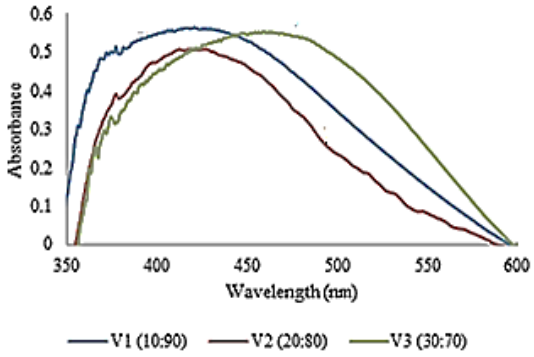

Figure 4. Effect of volume ratio of tridax daisy extract to 1mM $AgNO_3$ solution on AgNPs formation.

Using the tridax daisy extract, the trend in increasing absorbance peak with increasing ratio was not evident (Figure 4).All three ratios exhibited similar absorbance maxima with quite a broad band within the 400 to 460 nm range. Only a shift of absorbance peaks can be observed related to the particle size variation of the produced nanoparticles. The absorbances of the AgNPs as an effect of volume ratios are not significantly different, as shown in Table 1. Conclusively, a volume ratio of 10:90 can synthesize AgNPs using tridax daisy extract with an absorbance of 0.563.

The effect of pH in the silver nanoparticle synthesis was also studied (Figures 5 and 6). The initial pH of the tridax daisy and lemongrass extracts was about 4. After adding 1mM

AgNO3, the reaction mixture did not change color after 1 hour, indicating no formation of AgNPs. At pH 7, the color change was evident, and its SPR spectra showed maxima at 395 nm. An increase in absorbance and a red shift were observed in pH 9 at 401 nm and pH 11 at 405 nm. As discussed earlier, this redshift is attributed to the particle size increase. The optimum pH using lemongrass extract was pH 11 because it exhibited significantly higher absorbance (1.127) than pH 7 and pH 9 based on the statistical analysis performed.

The result above conforms with the study of Handayani, Ningrum, and Imawan [32] in which, at pH 11, a mixture of spherical and hexagonal-shaped AgNPs are formed with a Zeta potential of -16.1mV.

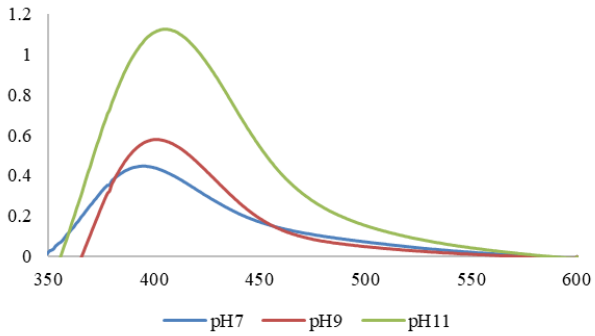

Figure 5. Effect of pH in the synthesis of AgNPs using lemongrass extract.

In the TD-AgNP synthesis, the trend in increasing absorbance with increasing pH is merely evident. The absorbance results using the three pH's were comparable, while the highest absorbance was shown in pH 9 (0.543). The absorbance maximum of pH 7 is located at 443 nm, and a blue shift to 432 at pH 9 and 413 at pH 11 was observed. The higher absorbance of pH 9 implies a greater concentration of AgNPs that can be produced; therefore, pH 9 was the optimum pH. The optimum pH in the synthesis of AgNPs is usually basic due to the presence of more OH^- ions, which assist in reducing silver ions [32].

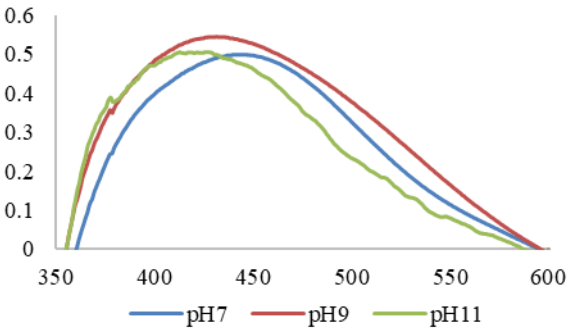

Figure 6. Effect of pH in the synthesis of AgNPs using tridax daisy extract.

The SPR spectra of AgNPs changed with temperature (Figures 7 and 8). In the synthesis using lemongrass leaf extract, the two temperatures used showed no significant difference statistically based on their absorbance spectra (Table 1). Though, the absorbance at approximately 410 nm at 50ºC (1.647) is still higher than that of 60ºC (1.528). Yong *et al*. [33] reported that at 65ºC, the formation of AgNPs was disrupted and was evident in the loss of spectral band and blackish color change due to the formation of Ag_2O. However, in this study, the black color change is still not evident at 60ºC. Because there is still a decrease in the

absorbance from 50ºC, the optimum temperature should be at 50ºC. Also, a slight blueshift from 410 nm at 50ºC to 406 nm at 60ºC was observed.

A similar trend was observed in the effect of temperature in the AgNP synthesis using tridax daisy extract. 50ºC was also the optimum temperature. A decrease in absorbance from 50ºC (0.486) to 60ºC (0.402) can be observed. However, a blueshift at 421 nm to 408 nm was detected, which indicates the formation of smaller AgNPs at 60ºC.

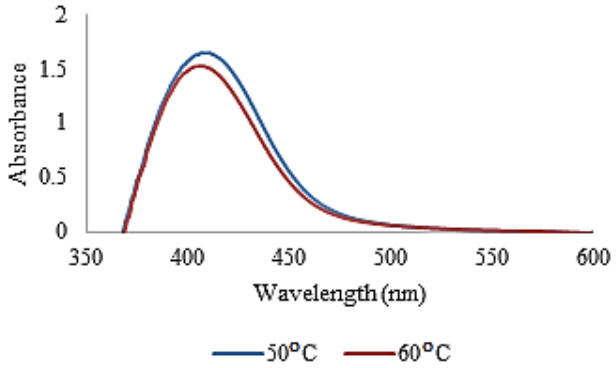

Figure 7. Effect of temperature in the synthesis of AgNPs using lemongrass extract.

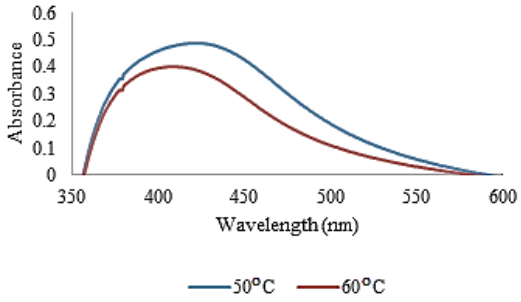

Figure 8. Effect of temperature in the synthesis of AgNPs using tridax daisy extract.

3.2.2. Copper nanoparticles.

The absorbances of copper nanoparticles synthesized from the lemongrass and tridax daisy extracts as affected by the different parameters are presented in Table 2. Volume ratio 1 exhibited a faint absorbance maximum at the CuNP characteristic wavelength at 584 nm. In comparison, it showed a relatively sharp peak at 428 nm (Figure 9), indicating the presence of Cu_2O and that the reduction process was incomplete. V2 and V3 statistically showed no difference in their absorbance peak at 577 nm and 581 nm, respectively. However, the optimum ratio is V2 because it displayed the highest absorbance (0.877), producing more CuNPs.

Table 2. Absorbances of CuNP from lemon grass and tridax daisy extracts.

Parameters		**LG-CuNP***	**TD-CuNP***
Volume Ratio	V1 (50:50)	0.286^b	0.531^b
	V2 (60:40)	0.877^a	0.999^a
	V3 (70:30)	0.805^a	0.761^a
pH	P1 (7)	0.161^b	0.164^b
	P2 (9)	0.285^b	1.031^a
	P3 (11)	0.690^a	1.011^a
Temperature	T1 (70ºC)	0.757^a	0.874^a
	T2 (80ºC)	0.875^a	0.592^a

* - absorbances in a column per parameter followed by the same letter superscript are not significantly different at 5% level.

A similar trend can be observed in the CuNP synthesis using tridax daisy extract. V1 and V2 showed similar spectra, having an absorbance peak at 592 nm and 584 nm. Both have an absorbance peak at around 420-430 nm, while in V3, a broad absorbance maximum was spotted at 547 nm, a significant blueshift from V1 and V3, and indicates dispersed sizes of the CuNPs (Figure 10, Table 2). The optimum ratio was the V2 because it displayed the highest absorbance at the CuNP fingerprint wavelength.

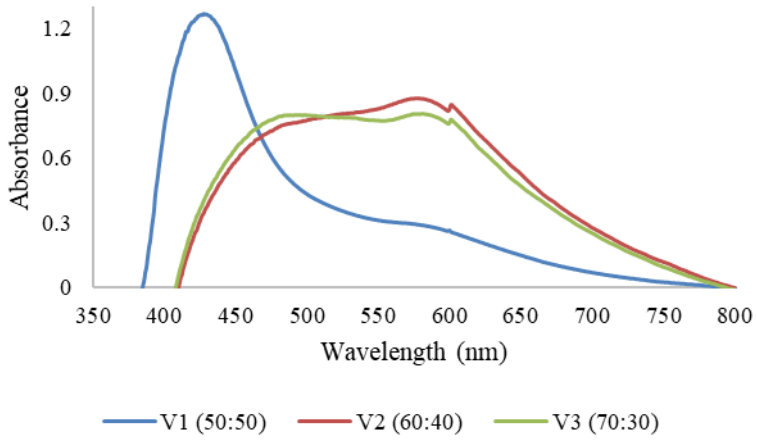

Figure 9. Effect of volume ratio of lemongrass extract to 1mM $CuSO_4.5H_2O$ solution on CuNPs formation.

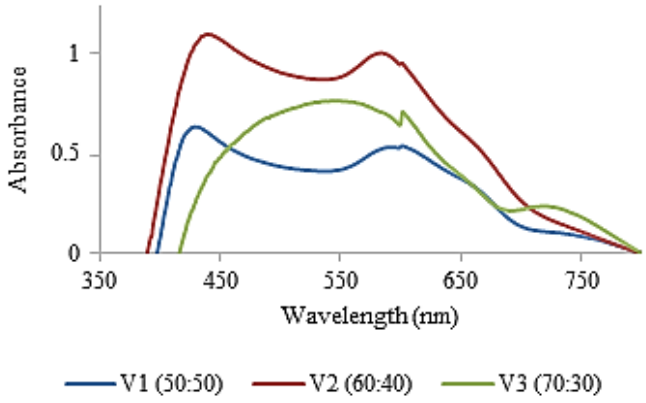

Figure 10. Effect of volume ratio of tridax daisy extracts to 1mM $CuSO_4.5H_2O$ solution on CuNPs formation.

The pH in aqueous media influences the reduction process in synthesizing copper nanoparticles [34].In the CuNP synthesis using lemongrass extract (Figure 11, Table 2), there is an increasing trend in the absorbance of the spectra from pH 7, pH 9, and pH 11 at the characteristic wavelength of CuNP. Plasmon resonance is evident for pH's from 7 to 11; the measured values were 592, 598, and 571 nm, respectively. The increasing trend of absorbance could be attributed to the increase in CuNP concentration, and the shifting of SPR peak to a specific wavelength depends on particle size, shape, solvent type, and capping agent [34]. Dang and colleagues [35] reported that at pH higher than 10 there is a decrease in the peak intensity around the maximum value. Yet, in this study, it was observed that the increase in pH from 9 to 11 exhibited a significant increase in the absorbance (Table 2) as more CuNPs were formed. Therefore, the optimum pH was pH 11. A similar result was reported by Zhang *et al*. [36], wherein using 0.5M of $NaBH_4$, pH 11 was optimized for forming ultrafine copper nanoparticles.

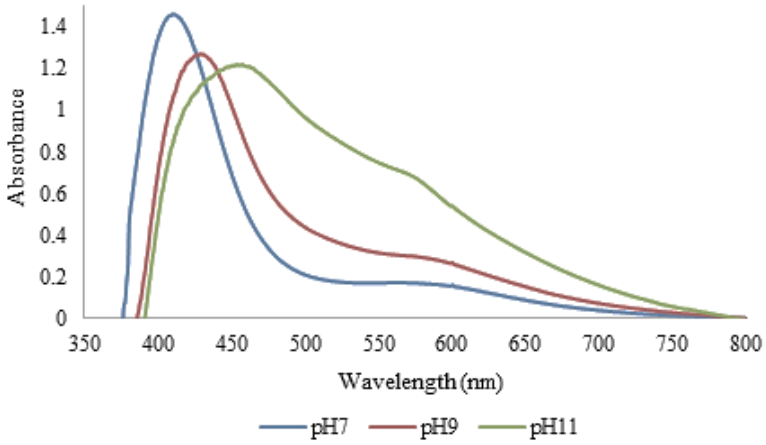

Figure 11. Effect of pH in the synthesis of CuNPs using lemongrass extract.

The increasing trend was not observed in the CuNP synthesis using tridax daisy extract (Figure 12). A faint absorbance maximum at 590 nm was noticed in pH 7, while similar absorbance was shown at pH 9 and pH 11 at 580 nm and 570 nm, respectively. The SPR peak of pH 9 has an absorbance of 1.031, which is not comparable to that of pH 11 (1.011) (Table 2), but still, the optimum pH is at pH 9 because it exhibited the highest absorbance at 570 nm. Furthermore, absorbance peaks around 400-450 nm were evident at the three pHs.

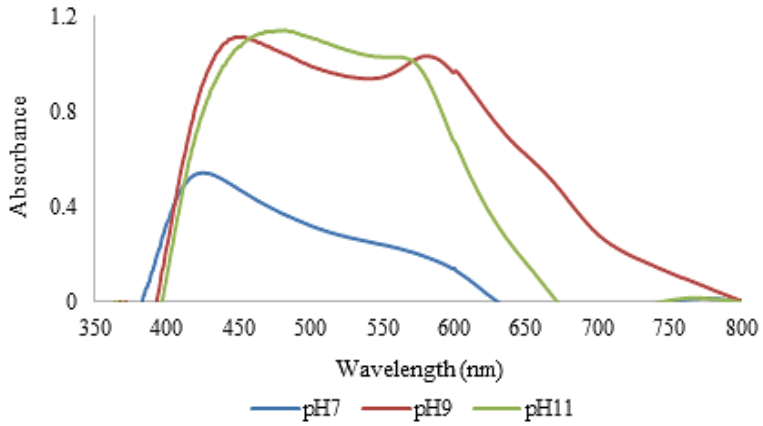

Figure 12. Effect of pH in the synthesis of CuNPs using tridax daisy extract.

It was observed that the synthesis of CuNPs is ideal at basic pH. At a trial synthesis that was done using the initial acidic condition, no color change was observed because the reduction of copper ions was improbable simultaneously, and CuNPs were found to be unstable [37].

In evaluating the effect of temperature in the synthesis of CuNPs, the other two parameters are controlled using the lemongrass and tridax daisy extracts. In the synthesis using lemongrass extracts (Figure 13 and Table 2), there is an increase from the absorbance of the SPR spectra of 70ºC to 80ºC. The absorbance maxima at 70ºC and 80ºC were located at 575 nm and 577 nm, respectively. Absorbance peaks at around 400-450 nm were not strongly evident. Based on the work of Khanna *et al*. [38], the presence of Cu_2O was evident at temperatures lower than 70ºC and if other appropriate conditions were not followed. Using the lemongrass extract, the optimum temperature was at 80ºC.

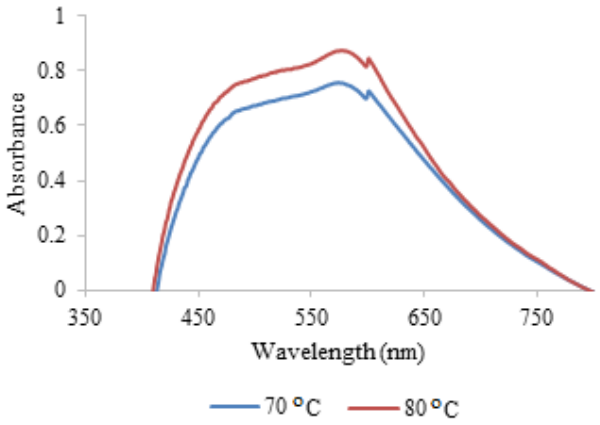

Figure 13. Effect of temperature in the synthesis of CuNPs using lemon grass extract.

In contrast to the report of Khanna *et al*. [38], using the tridax daisy extract in the CuNP synthesis (Figure 14), the absorbance maxima of Cu_2O were present at both 70ºC and 80ºC. The phenomenon could be attributed to other conditions, such as a lack of stabilizing and capping agents or incomplete reduction. The absorbance peaks are around 570 nm for 70ºC and 80ºC. Meanwhile, the optimum temperature is 70ºC because it exhibited higher absorbance in the SPR spectra than 80ºC.

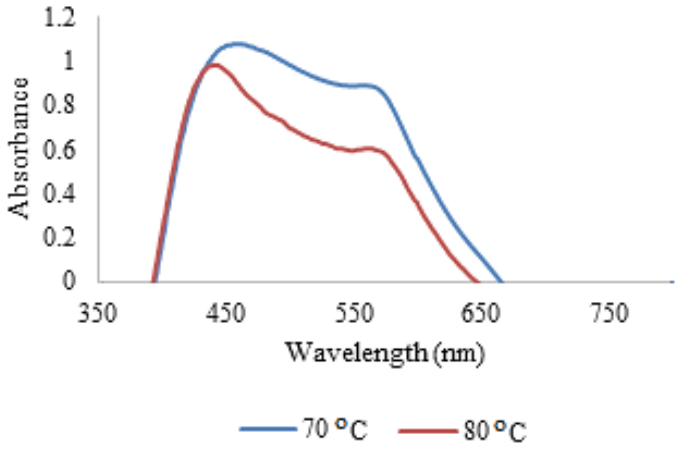

Figure 14. Effect of temperature in the synthesis of CuNPs using tridax daisy extract.

3.3. Size and morphological structure.

3.3.1. Silver nanoparticles.

The SPR spectra often indicate the size of the produced silver nanoparticles [38]. Using the spectra of the synthesized AgNPs following the optimized parameters, the SPR peaks were found to be at 422 nm (LG-AgNPs) and 432 nm (TD-AgNPs). These SPR bands characteristic of silver nanoparticles were presumed to correspond to fine nanoparticles with a size of 35-60 nm [39].

By magnifying the samples x20000 and x35000 using a Scanning Electron Microscope (SEM), agglomerates of AgNPs can be seen in representative samples of synthesized AgNP using lemongrass extract (Figure 15A) and tridax daisy extract (Figure 15B). Due to magnification limitations, only the spherical shape of AgNPs could be confirmed as they are

present in clusters. Jha and Prasad [40] observed the same spherical shapes of the synthesized AgNPs using *Cycas* leaf broth.

Further image analysis by measuring the size of 100 representative AgNPs, using the ImageJ image processing program revealed a size distribution of 36-109 nm for LG-AgNPs, having a mean length of 73 ± 18 nm (Figure 15A) and 32-106 nm for TD-AgNPs, having a mean length of 70 ± 16 nm (Figure 15B). The determined sizes didn't reach the previous 35-60 nm assumption.

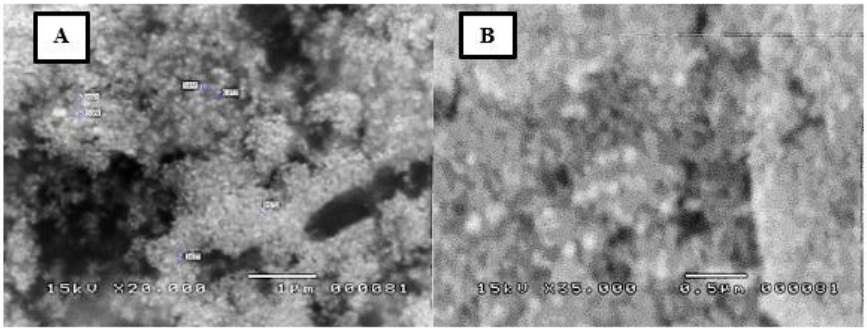

Figure 15. SEM images of AgNPs synthesized using (A) lemongrass and (B) tridax daisy extracts.

3.3.2. Copper nanoparticles.

Using the spectra of the synthesized CuNPs following the optimized parameters, the SPR peaks were found to be at 577 nm (LG-AgNPs) and 580 nm (TD-AgNPs). Park *et al*. [41] reported that the observed size of CuNPs synthesized by the polyol method with SPR peak around 560-570 nm is 14-50 nm. Therefore at 577 nm and 580 nm, we could assume smaller sizes of CuNPs.

In the SEM images, agglomerates of spherical and irregularly-shaped CuNPs can be observed from representative samples of CuNPs synthesized using lemongrass extract (Figure 16A) and tridax daisy extract (Figure 16B).

Using the ImageJ image processing program, the selected 100 representative CuNPs showed a size distribution of 32-95 nm for LG-CuNPs, having a mean length of 57 ± 15 nm (Figure 4.5.2.2a), and 31-87 nm for TD-CuNPs, having a mean length of 58 ± 13 nm (Figure 4.5.2.2b).

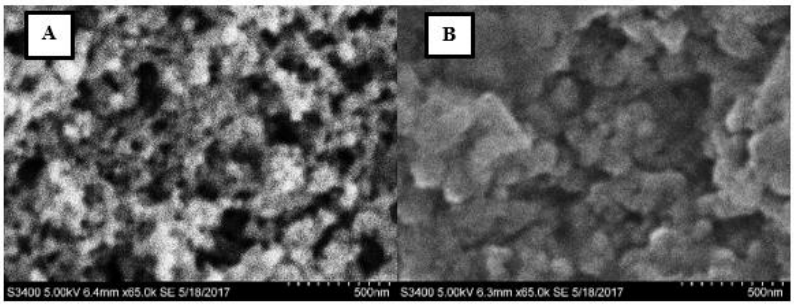

Figure 16. SEM images of CuNPs synthesized using (A) lemongrass extract and (B) tridax daisy extract.

3.4. Anti-fruit fly test.

The potential anti-fruit fly activity of the solvent, which served as the control plant extracts and plant extracts-metal nanoparticles, was evaluated (Figure 17) in three replicate treatments containing five male fruit flies each.

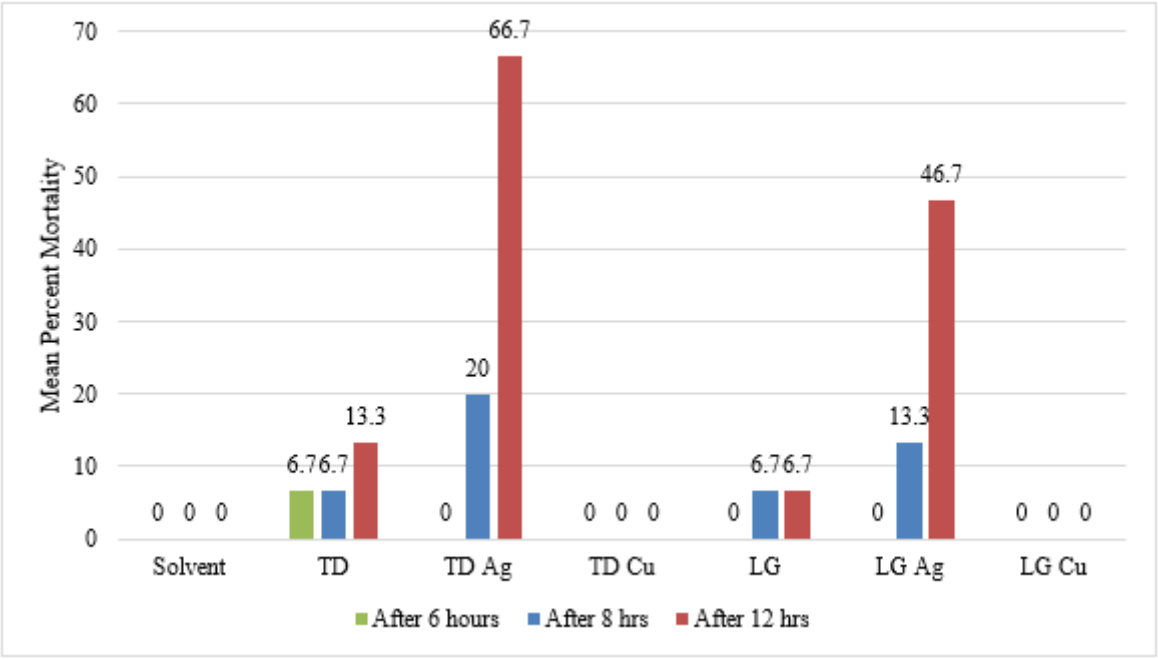

Figure 17. Mean percent mortality of fruit flies after progressive hours of exposure to different treatments.

All the treatments showed no anti-fruit fly activity until the fruit flies were exposed to the treatments for 6 hours. Only the fruit flies exposed to tridax daisy after 6 hours exhibit 6.7 ± 11.5% mortality but is not significantly more effective than the other treatments. After 8 hours of exposure, the TD-AgNP treatment caused 20.0 ± 20.0% mortality, and the LG-AgNP treatment caused 13.3 ± 11.5% mortality. However, the effectiveness of the treatments was significantly the same at 8 hours of exposure (Table 3). After the 12-hour exposure, the TD-AgNP treatment showed significant improvement in the anti-fruit fly activity compared to the tridax daisy extract, from 13.3 ± 11.5% to 66.7 ± 23.1%, and the LG-AgNP treatment also exhibited a significant increase compared to the lemongrass extract, from 6.7 ± 11.5% to 46.7 ± 30.5% (Table 3). Furthermore, the effectiveness of the two AgNP treatments was comparable, despite the higher percent mortality exhibited by TD-AgNP. A similar observation was stated by Egunyomi, Gbadamosi, and Osiname [42], in which tridax daisy extract showed a greater effect than lemongrass extract in controlling *Anopheles stephensi*, but is not significantly more effective. Paragas, Cruz, and Fiegalan [43] reported that the aqueous lemongrass extract showed only 26.67% mortality after exposing the fruit flies for 24 hours.

Table 3. Statistical comparison of the percent mortality of fruit flies after progressive hours of exposure to different treatments.

Time (hr)	Mean Percent Mortality						
	Solvent	Tridax Daisy			Lemongrass		
		Extract	AgNP	CuNP	Extract	AgNP	CuNP
0.5	0.0	0.0	0.0	0.0	0.0	0.0	0.0
1.0	0.0	0.0	0.0	0.0	0.0	0.0	0.0
2.0	0.0	0.0	0.0	0.0	0.0	0.0	0.0
4.0	0.0	0.0	0.0	0.0	0.0	0.0	0.0
6.0	0.0^{a}	6.7^{a}	0.0^{a}	0.0^{a}	0.0^{a}	0.0^{a}	0.0^{a}
8.0	0.0^{a}	6.7^{a}	20.0^{a}	0.0^{a}	6.7^{a}	13.3^{a}	0.0^{a}
12.0	0.0^{b}	13.3^{b}	66.7^{a}	0.0^{b}	6.7^{b}	46.7^{a}	0.0^{b}

*Means within the same row with the same superscript are not significantly different.

As previously reported, the anti-fruit fly activity of the tridax daisy and lemongrass extract could be attributed to the presence of phenolics, flavonoids, and alkaloids [44]. These

metabolites were also present in basil oil, which exhibited insecticidal activity against *Bactrocera dorsalis*, *Bactrocera cucurbitae*, and *Ceratitis capitata* [45].

Hyperactivity was observed in the first few hours after the fruit flies were exposed to effective treatments. After about 4 to 6 hours, the fruit flies' mobility was depleted. Rattan [46] reported that the hyperactivity was possibly due to neuroexcitation. The slow mobility could be due to energy depletion, neuromuscular fatigue, and neuroinhibition by possible oxygen deprivation and reduced respiratory capacity, possibly leading to mortality. Armstrong *et al*. [47] reported that AgNPs, as consumed by *Drosophila melanogaster*, a dipteran insect such as *Bactrocera dorsalis*, inhibited membrane-bound copper-transporters, resulting in intracellular copper depletion. Silver nanoparticles also caused the reduction of tyrosine hydroxylase activity in animal brain [48], and reduce adult locomotive activity and reproductive development in *Drosophila* [49].

Meanwhile, the two CuNP-based treatments showed no anti-fruit fly effect after 12 hours of exposure. A decline in the anti-fruit fly activity of the two plant extracts was found. As reported by Muttkowski [50], copper is essential to the physiological activity of arthropods due to its role in hemocyanin. This respiratory protein transports oxygen throughout the bodies of some invertebrates. Thus the lack of the anti-fruit fly activity of CuNPs could be due to the very low concentration of CuNPs consumed by the fruit flies.

For a possible application, since dose-dependent toxicity of silver nanoparticles in human cells is reported in some studies [51], it is essential to disregard treating the AgNP-based tridax daisy extract employing sprays to avoid contact of AgNPs to fruits. Thus, effective treatment could be incorporated with pest management techniques, such as using bait stations with natural attractants.

4. Conclusions

Based on the results of this study, silver and copper nanoparticles can be formed using lemongrass and tridax daisy coconut water extracts. The success of synthesizing AgNPs and CuNPs depends on the volume ratio of the extract to silver/copper salt solution. The formation of AgNPs and CuNPs using lemongrass extract is favored by a reaction pH of 11 and pH of 9 using tridax daisy extract. The synthesis of AgNPs requires an optimum temperature of 50ºC, while the synthesis of CuNPs requires a temperature not lower than 70ºC. Silver nanoparticles present in agglomerates with an approximate length of 70-73 nm and copper nanoparticles with an average length range of 57-58 nm can be similarly formed using lemon grass and tridax daisy extracts. Silver nanoparticles synthesized from tridax daisy extract exhibit the highest potential in controlling oriental fruit flies. Copper nanoparticles showed no potential insecticidal activity against oriental fruit flies. Secondary metabolites in the plant extracts are responsible for reducing metal ions to metal nanoparticles and their potential anti-fruit fly activities.

Funding

This research received no external funding.

Acknowledgments

The authors want to acknowledge the support of the Department of Science and Technology (DOST) and the Bank of Philippine Islands (BPI).

Conflicts of Interest

The authors declare no conflict of interest.

References

1. Susanto, A.; Permana, A.D.; Subahar, T.S.; Soesilohadi, R.C.H.; Leksono, A.S.; Fernandes, A.A.R. Population dynamics and projections of fruit flies Bactrocera dorsalis and B. carambolae in Indonesian mango plantation. *Agriculture and Natural Resources* **2022**, *56*, 169–179.
2. Mutamiswa, R.; Nyamukondiwa, C.; Chikowore, G.; Chidawanyika, F. Overview of oriental fruit fly, Bactrocera dorsalis (Hendel)(Diptera: Tephritidae) in Africa: From invasion, bio-ecology to sustainable management. *Crop Protection* **2021**, *141*, https://doi.org/10.1016/j.cropro.2020.105492.
3. Mazumdar, S.; Hebert, P. A survey of True flies (Insecta: Diptera) by DNA Barcoding of Malaise Trap Collection in Bangladesh. *Journal of Insect Biodiversity and Systematics* **2021**, *7*, https://doi.org/10.52547/jibs.7.1.15.
4. de Graaf, L.; Boulanger, M.; Bureau, M.; Bouvier, G.; Meryet-Figuiere, M.; Tual, S.; Lebailly, P.; Baldi, I. Occupational pesticide exposure, cancer and chronic neurological disorders: A systematic review of epidemiological studies in greenspace workers. *Environ Res* **2022**, *203*, https://doi.org/10.1016/j.envres.2021.111822.
5. Kirkhorn, S.R.; Schenker, M.B. Current health effects of agricultural work: respiratory disease, cancer, reproductive effects, musculoskeletal injuries, and pesticide-related illnesses. *Journal of agricultural safety and health* **2002**, *8*, 199-214, https://doi.org/10.13031/2013.8432.
6. Broumas, T.; Haniotakis, G.; Liaropoulos, C.; Tomazou, T.; Ragoussis, N. The efficacy of an improved form of the mass-trapping method, forthe control of the olive fruit fly, Bactrocera oleae (Gmelin) (Dipt., Tephritidae): pilot-scale feasibility studies. *Journal of Applied Entomology* **2002**, *126*, 217-223, https://doi.org/10.1046/j.1439-0418.2002.00637.x.
7. Jatav, K.S.; Dhar, J. Hybrid approach for pest control with impulsive releasing of natural enemies and chemical pesticides: A plant–pest–natural enemy model. *Nonlinear Analysis: Hybrid Systems* **2014**, *12*, 79-92, https://doi.org/10.1016/j.nahs.2013.11.011.
8. Klungness, L.M.; Jang, E.B.; Mau, R.F.; Vargas, R.I.; Sugano, J.S.; Fujitani, E. New sanitation techniques for controlling tephritid fruit flies (Diptera: Tephritidae) in Hawaii. *J. Appl. Sci. Environ. Manag.* **2005**, *9*, 5-14.
9. Kumar, P.; Kamle, M.; Borah, R.; Mahato, D.K.; Sharma, B. Bacillus thuringiensis as microbial biopesticide: uses and application for sustainable agriculture. *Egyptian Journal of Biological Pest Control* **2021**, *31*, 1-7, https://doi.org/10.1186/s41938-021-00440-3.
10. Menzler-Hokkanen, I.; Ruhanen, H.; Hokkanen, H.M.T. Mortality of the oriental fruit fly, Bactrocera dorsalis, during pupation in insect pest suppressive soils. *Entomologia Experimentalis et Applicata* **2022**, *170*, 565-572, https://doi.org/10.1111/eea.13176.
11. Prokopy, R.J.; Miller, N.W.; Piñero, J.C.; Barry, J.D.; Tran, L.C.; Oride, L.; Vargas, R.I. Effectiveness of GF-120 Fruit Fly Bait Spray Applied to Border Area Plants for Control of Melon Flies (Diptera: Tephritidae). *Journal of Economic Entomology* **2003**, *96*, 1485-1493, https://doi.org/10.1603/0022-0493-96.5.1485.
12. Thomas, D.B.; Mangan, R.L. Nontarget impact of spinosad GF-120 bait sprays for control of the Mexican fruit fly (Diptera: Tephritidae) in Texas citrus. *J Econ Entomol* **2005**, *98*, 1950-1956, https://doi.org/10.1603/0022-0493-98.6.1950.
13. Hajji-Hedfi, L.; Chhipa, H. Nano-based pesticides: challenges for pest and disease management. *Euro-Mediterranean Journal for Environmental Integration* **2021**, *6*, 1-8, https://doi.org/10.1007/s41207-021-00279-y.
14. Wang, D.; Saleh, N.B.; Byro, A.; Zepp, R.; Sahle-Demessie, E.; Luxton, T.P.; Ho, K.T.; Burgess, R.M.; Flury, M.; White, J.C.; Su, C. Nano-enabled pesticides for sustainable agriculture and global food security. *Nature Nanotechnology* **2022**, *17*, 347-360, https://doi.org/10.1038/s41565-022-01082-8.
15. Deka, B.; Babu, A.; Baruah, C.; Barthakur, M. Nanopesticides: a systematic review of their prospects with special reference to tea pest management. *Front. Nutr.* **2021**, *8*, https://doi.org/10.3389/fnut.2021.686131.
16. Deka, B.; Nisha, S.N.; Baruah, C.; Babu, A.; Sarkar, S.; Phukan, H. Agricultural Pest Management with Plant-Derived Nanopesticides: Prospects and Challenges. *J. Appl. Nanotechnol.* **2022**, *1*, 1-9.
17. Kookana, R.S.; Boxall, A.B.A.; Reeves, P.T.; Ashauer, R.; Beulke, S.; Chaudhry, Q.; Cornelis, G.; Fernandes, T.F.; Gan, J.; Kah, M.; Lynch, I.; Ranville, J.; Sinclair, C.; Spurgeon, D.; Tiede, K.; Van den Brink, P.J. Nanopesticides: Guiding Principles for Regulatory Evaluation of Environmental Risks. *Journal of Agricultural and Food Chemistry* **2014**, *62*, 4227-4240, https://doi.org/10.1021/jf500232f.
18. Malik, A.; Shayesta, I.; Mushtaq, A.M.; Zaffar Mahdi, D.; Amjad, M.; Saima, S.; Bisma, R.; Showkat, S. Nano Pesticides Application in Agriculture and their Impact on Environment. In: *Agricultural Development in Asia-Potential Use of Nano-Materials and Nanotechnology*. IntechOpen **2021**.

19. Tleuova, A.B.; Wielogorska, E.; Talluri, V.S.S.L.P.; Štěpánek, F.; Elliott, C.T.; Grigoriev, D.O. Recent advances and remaining barriers to producing novel formulations of fungicides for safe and sustainable agriculture. *Journal of Controlled Release* **2020**, *326*, 468-481, https://doi.org/10.1016/j.jconrel.2020.07.035.
20. Okey-Onyesolu, C.F.; Hassanisaadi, M.; Bilal, M.; Barani, M.; Rahdar, A.; Iqbal, J.; Kyzas, G.Z. Nanomaterials as Nanofertilizers and Nanopesticides: An Overview. *ChemistrySelect* **2021**, *6*, 8645-8663, https://doi.org/10.1002/slct.2021102379.
21. Makarov, V.V.; Love, A.J.; Sinitsyna, O.V.; Makarova, S.S.; Yaminsky, I.V.; Taliansky, M.E.; Kalinina, N.O. "Green" nanotechnologies: synthesis of metal nanoparticles using plants. *Acta naturae* **2014**, *6*, 35-44.
22. Cele, T. Preparation of nanoparticles. In: *Engineered Nanomaterials-Health and* Safety. Avramescu, S.M.; Akhtar, K.; Fierascu, I.; Khan, S.B.; Ali, F.; Asiri, A.M. IntechOpen, **2020**.
23. Masurkar, S.A.; Chaudhari, P.R.; Shidore, V.B.; Kamble, S.P. Rapid Biosynthesis of Silver Nanoparticles Using Cymbopogan Citratus (Lemongrass) and its Antimicrobial Activity. *Nano-Micro Letters* **2011**, *3*, 189-194, http://dx.doi.org/10.3786/nml.v3i3.p189-194.
24. Bhati–Kushwaha, H.; Malik, C. Biosynthesis of silver nanoparticles using fresh extracts of Tridax procumbens Linn. *Indian J. Exp. Biol.* **2014**, *52*, 359-368.
25. Xia, Y.; Campbell, D.J. Plasmons: Why Should We Care? *Journal of Chemical Education* **2007**, *84*, https://doi.org/10.1021/ed084p91.
26. Mulfinger, L.; Solomon, S.D.; Bahadory, M.; Jeyarajasingam, A.V.; Rutkowsky, S.A.; Boritz, C. Synthesis and Study of Silver Nanoparticles. *Journal of Chemical Education* **2007**, *84*, https://doi.org/10.1021/ed084p322.
27. Kanhed, P.; Birla, S.; Gaikwad, S.; Gade, A.; Seabra, A.B.; Rubilar, O.; Duran, N.; Rai, M. In vitro antifungal efficacy of copper nanoparticles against selected crop pathogenic fungi. *Materials Letters* **2014**, *115*, 13-17, https://doi.org/10.1016/j.matlet.2013.10.011.
28. Nasrollahzadeh, M.; Sajadi, S.M.; Khalaj, M. Green synthesis of copper nanoparticles using aqueous extract of the leaves of Euphorbia esula L and their catalytic activity for ligand-free Ullmann-coupling reaction and reduction of 4-nitrophenol. *RSC Advances* **2014**, *4*, 47313-47318, https://doi.org/10.1039/C4RA08863H.
29. Chen, L.; Zhang, Y.; Zhu, P.; Zhou, F.; Zeng, W.; Lu, D. D.; Sun, R.; & Wong, C. Copper salts mediated morphological transformation of Cu_2O from cubes to hierarchical flower-like or microspheres and their supercapacitors performances. *Sci. Rep.* **2015**, *5*, https://doi.org/10.1038/srep09672.
30. Blosi, M.; Albonetti, S.; Dondi, M.; Martelli, C.; Baldi, G. Microwave-assisted polyol synthesis of Cu nanoparticles. *Journal of Nanoparticle Research* **2011**, *13*, 127-138, https://doi.org/10.1038/srep09672.
31. Wang, L.; Hasanzadeh Kafshgari, M.; Meunier, M. Optical Properties and Applications of Plasmonic-Metal Nanoparticles. *Advanced Functional Materials* **2020**, *30*, https://doi.org/10.1002/adfm.202005400.
32. Handayani, W.; Ningrum, A.S.; Imawan, C. The role of pH in synthesis silver nanoparticles using pometia pinnata (matoa) leaves extract as bioreductor. *Journal of Physics: Conference Series IOP Publishing* **2020**, *1428*, https://doi.org/10.1088/1742-6596/1428/1/012021.
33. Yong, N.L.; Ahmad, A.; Mohammad, A.W. Synthesis and characterization of silver oxide nanoparticles by a novel method. *Int. J. Sci. Eng. Res.* **2013**, *4*, 155-158.
34. Sarwar, N.; Humayoun, U.B.; Kumar, M.; Zaidi, S.F.A.; Yoo, J.H.; Ali, N.; Jeong, D.I.; Lee, J.H.; Yoon, D.H. Citric acid mediated green synthesis of copper nanoparticles using cinnamon bark extract and its multifaceted applications. *Journal of Cleaner Production* **2021**, *292*, https://doi.org/10.1016/j.jclepro.2021.125974.
35. Dang, T.M.D.; Le, T.T.T.; Fribourg-Blanc, E.; Dang, M.C. Synthesis and optical properties of copper nanoparticles prepared by a chemical reduction method. *Advances in Natural Sciences: Nanoscience and Nanotechnology* **2011**, *2*, https://doi.org/10.1088/2043-6262/2/1/015009.
36. Zhang, H.-X.; Siegert, U.; Liu, R.; Cai, W.-B. Facile Fabrication of Ultrafine Copper Nanoparticles in Organic Solvent. *Nanoscale Research Letters* **2009**, *4*, https://doi.org/10.1007/s11671-009-9301-2.
37. Joshi, S.S.; Patil, S.F.; Iyer, V.; Mahumuni, S. Radiation induced synthesis and characterization of copper nanoparticles. *Nanostructured Materials* **1998**, *10*, 1135-1144, https://doi.org/10.1016/S0965-9773(98)00153-6.
38. Khanna, P.K.; More, P.; Jawalkar, J.; Patil, Y.; Koteswar Rao, N. Synthesis of hydrophilic copper nanoparticles: effect of reaction temperature. *Journal of Nanoparticle Research* **2009**, *11*, 793-799, https://doi.org/10.1007/s11051-008-9441-9.
39. Kelly, K.L.; Coronado, E.; Zhao, L.L.; Schatz, G.C. The Optical Properties of Metal Nanoparticles: The Influence of Size, Shape, and Dielectric Environment. *The Journal of Physical Chemistry B* **2003**, *107*, 668-677, https://doi.org/10.1021/jp026731y.
40. Jha, A.K.; Prasad, K. Green Synthesis of Silver Nanoparticles Using Cycas Leaf. *International Journal of Green Nanotechnology: Physics and Chemistry* **2010**, *1*, P110-P117, https://doi.org/10.1080/19430871003684572.
41. Park, B.K.; Jeong, S.; Kim, D.; Moon, J.; Lim, S.; Kim, J.S. Synthesis and size control of monodisperse copper nanoparticles by polyol method. *Journal of Colloid and Interface Science* **2007**, *311*, 417-424, https://doi.org/10.1016/j.jcis.2007.03.039.

42. Egunyomi, A.; Gbadamosi, I. T.; & Osiname, K. O. Comparative effectiveness of ethnobotanical mosquito repellents used in Ibadan, Nigeria. *J. Appl. Biosci* **2010**, *36*, 2383-2388.
43. Paragas, D. S.; Cruz, K. D.; & Fiegalan, E. R. Screening of plants for insecticidal activities against oriental fruit fly Bactrocera dorsalis (Hendel) for pest management of mango Mangifera indica. *Malaysian Journal of Analytical Sciences* **2020**, *24*, 615-629.
44. Salaria, D.; Rolta, R.; Sharma, N.; Patel, C.N.; Ghosh, A.; Dev, K.; Sourirajan, A.; Kumar, V. In vitro and in silico antioxidant and anti-inflammatory potential of essential oil of Cymbopogon citratus (DC.) Stapf. of North-Western Himalaya. *Journal of Biomolecular Structure and Dynamics* **2022**, *40*, 14131-14145, https://doi.org/10.1080/07391102.2021.2001371.
45. Chang, C.L.; Cho, I.K.; Li, Q.X. Insecticidal activity of basil oil, trans-anethole, estragole, and linalool to adult fruit flies of Ceratitis capitata, Bactrocera dorsalis, and Bactrocera cucurbitae. *J. Econ. Entomol.* **2009**, *102*, 203-209, https://doi.org/10.1603/029.102.0129.
46. Rattan, R.S. Mechanism of action of insecticidal secondary metabolites of plant origin. *Crop Protection* **2010**, *29*, 913-920, https://doi.org/10.1016/j.cropro.2010.05.008.
47. Armstrong, N.; Ramamoorthy, M.; Lyon, D.; Jones, K.; Duttaroy, A. Mechanism of Silver Nanoparticles Action on Insect Pigmentation Reveals Intervention of Copper Homeostasis. *PLOS ONE* **2013**, *8*, https://doi.org/10.1371/journal.pone.0053186.
48. Janzadeh, A.; Behroozi, Z.; saliminia, F.; Janzadeh, N.; Arzani, H.; Tanha, K.; Hamblin, M.R.; Ramezani, F. Neurotoxicity of silver nanoparticles in the animal brain: a systematic review and meta-analysis. *Forensic Toxicology* **2022**, *40*, 49-63, https://doi.org/10.1007/s11419-021-00589-4.
49. Pendleton, R.G.; Rasheed, A.; Hillman, R. Effects of adrenergic agents on locomotor behavior and reproductive development in Drosophila. *Drug Development Research* **2000**, *50*, 142-146, https://doi.org/10.1002/1098-2299(200006)50:2<142::AID-DDR2>3.0.CO;2-7.
50. Muttkowski, R. A. Copper: its occurrence and rôle in insects and other animals. *Transactions of the American Microscopical Society* **1921**, *40*, 144-157, https://doi.org/10.2307/3221584.
51. Kim, S.; Choi, J.E.; Choi, J.; Chung, K.-H.; Park, K.; Yi, J.; Ryu, D.-Y. Oxidative stress-dependent toxicity of silver nanoparticles in human hepatoma cells. *Toxicology in Vitro* **2009**, *23*, 1076-1084, https://doi.org/10.1016/j.tiv.2009.06.001.